molecular pharmaceutics

BRIEF ARTICLE

pubs.acs.org/molecularpharmaceutics

Subtraction of DC Conductivity and Annealing: Approaches To Identify Johari−Goldstein Relaxation in Amorphous Trehalose

Sunny P. Bhardwaj and Raj Suryanarayanan*

Department of Pharmaceutics, University of Minnesota, Minneapolis, Minnesota 55455, United States

Supporting Information

ABSTRACT: Amorphous trehalose finds extensive use as a stabilizer of biomolecules including proteins and phospholipids. Hypothesizing that molecular mobility is a determinant of its stability, dynamic dielectric spectroscopy (DDS) was used to map the different modes of mobility. Isothermal dielectric relaxation profiles of amorphous trehalose were obtained, over the frequency range of 10^{-1}−10^{7} Hz, and at temperatures ranging from 30−170 °C. At temperatures close to the glass transition (T_g), the α-relaxation was not readily discernible due to interference from dc conductivity. We used Kramers−Kronig transformation that enabled not only the complete resolution of α-relaxation but also the identification of an excess wing, in the high frequency tail of α-relaxation. On annealing, this excess wing developed into a partially resolved and hitherto unidentified β-relaxation peak. This peak, due to its position in the dielectric spectrum, its annealing time dependence and the good agreement with the calculated independent relaxation time, was assigned to the Johari−Goldstein process. This work demonstrates the utility of conductivity subtraction coupled with sub-T_g annealing to successfully study all the modes of mobility in amorphous trehalose. This approach can potentially be extended to situations wherein dc conductivity impedes the complete characterization of molecular mobility.

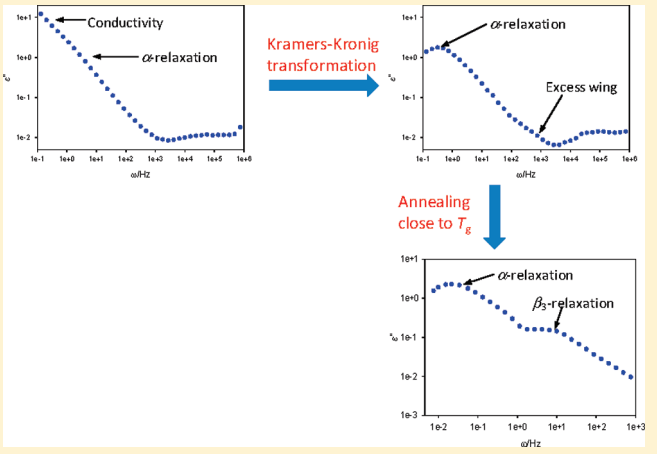

KEYWORDS: trehalose, dielectric spectroscopy, molecular mobility, Kramers−Kronig, annealing, Johari−Goldstein relaxation

INTRODUCTION

In light of the very poor aqueous solubility of numerous drug candidates under development, amorphization is increasingly emerging as a possible strategy for solubility enhancement.[1] However, the increased free energy of an amorphous compound, when compared with its crystalline counterpart, can also result in decreased physical stability, manifested by the tendency to crystallize. Molecular mobility, an extensively studied property of amorphous materials, can be a major determinant of stability.[2,3] A correlation between global molecular mobility (i.e., α-relaxation) and physical stability has been documented in many amorphous materials.[4−6] Therefore, a reduction in molecular mobility has often been suggested as a strategy for improving physical stability. Recently, several studies have shown the possible role of secondary relaxations in the physicochemical stability of amorphous materials. Local mobility involves fast noncooperative motions arising from the orientation of individual molecules or their parts.[7−9] These local motions are also referred to as β-relaxations. Evidence of crystallization at temperatures far below T_g and crystallization tendencies not explained by structural relaxation time are two indirect observations which have strongly hinted at the importance of local mobility.[10−13] Although there can be many secondary relaxations, often the slowest β-relaxation, referred to as the Johari−Goldstein (JG) relaxation, has received the most attention in literature .[14,15] In addition to its potential role in governing stability, JG relaxation may also be a precursor to global mobility.[16,17]

Many instrumental techniques such as differential scanning calorimetry (DSC),[18,19] dielectric spectroscopy,[4,5] shear viscosity measurement[20] and nuclear magnetic relaxation time measurement[6,21] have been employed to study molecular mobility in amorphous materials. Dynamic dielectric spectroscopy (DDS) is a technique that enables a "mapping" of the different modes of mobility over a wide range of temperatures.[22,23] It offers unique advantages in that it not only can distinguish between local and global mobility but can even differentiate one secondary relaxation from another. In fact, it has been the most successful technique to study secondary relaxations in a variety of materials.[9,11,14,15,24] One major drawback, as was found in many sugars and polyalcohols, is the contribution of ionic or dc conductivity to the imaginary part of complex permittivity or dielectric loss.[25,26] This can potentially

Received: January 12, 2011
Accepted: June 4, 2011
Revised: May 31, 2011
Published: June 04, 2011

interfere with the characterization of α-relaxation, if both occur in the same frequency region.[24,25] In such situations, there are two possible approaches to analyze the underlying relaxation. If the α-relaxation peak is discernible as a shoulder in the steep conductivity, the Havriliak−Negami model which takes into consideration both relaxation and dc conductivity can be used to fit this region of dielectric spectrum (eq 1).

$$\varepsilon^*(\omega) = \left[\varepsilon_\infty + \frac{\Delta\varepsilon}{(1 + (i\omega\tau)^{\beta_{HN}})^{\gamma_{HN}}}\right] + \frac{\sigma_0}{i\varepsilon_s\omega} \quad (1)$$

$$\varepsilon^*(\omega) = \varepsilon'(\omega) - \varepsilon''(\omega) \quad (2)$$

where $\varepsilon^*(\omega)$ is the complex dielectric permittivity comprising of a real part $\varepsilon'(\omega)$ and an imaginary part $\varepsilon''(\omega)$, ω is the frequency, τ is the relaxation time, σ_0 is the dc conductivity and $\Delta\varepsilon$ is the dielectric strength given by $(\varepsilon_s - \varepsilon_\infty)$, where ε_s is the static permittivity or the low frequency limit $(\omega\rightarrow 0)$ of $\varepsilon'(\omega)$ and ε_∞ is the high frequency limit $(\omega\rightarrow\infty)$ of $\varepsilon'(\omega)$. β_{HN} is a parameter describing symmetric peak broadening with $0 < \beta < 1$ while γ_{HN} is the asymmetric broadening parameter with $0 < \gamma < 1$.

However, in light of the potentially serious errors due to fitting, such an approach has not found widespread use. The second possible strategy is to use the Kramers−Kronig relation or the so-called Hilbert transform.[25−27] This relation links the real (dielectric constant, ε') and the imaginary (dielectric loss, ε'') parts of the complex dielectric permittivity ε^*. If the dielectric constant is known at two frequencies (ω_1 and ω_2), one can calculate the dielectric loss at the median frequency (logarithmic scale) using the derivative form of the Kramers−Kronig relation (eq 3). When there is no contribution of interfacial polarization to the permittivity, the dielectric constant has contributions only from relaxation processes. In such cases, only dc conductivity contributes to dielectric loss.

$$\varepsilon'' \approx \frac{\pi}{2}\frac{\varepsilon'(\omega_1) - \varepsilon'(\omega_2)}{\ln\left(\frac{\omega_2}{\omega_1}\right)} \quad (3)$$

Trehalose (α-D-glucopyranosyl α-D-glucopyranoside) finds extensive use as a stabilizer of biomolecules including proteins and phospholipids.[28,29] This protective property is believed to be due to its rigid glassy state and its ability to act as a "water substitute".[30] Accordingly, the amorphous form of trehalose has been the subject of many investigations. It exhibits many interesting properties including a high glass transition temperature ($T_g \sim 117$ °C) and relatively low crystallization tendency. However, recently, crystallization of trehalose was observed during freeze-drying.[31,32] Since the amorphous state is a necessary (though not sufficient) condition for its ability to serve as a bioprotective and a stabilizer, its crystallization behavior warrants serious investigation.

Molecular mobility in amorphous trehalose, our compound of interest, has received only limited attention in the literature.[24,25,33−35] Because of the conductivity interference, until recently, α-relaxation in trehalose could not be monitored by dielectric spectroscopy, at temperatures close to T_g. Earlier this year, based on fitting the dielectric loss data, Kwon et al. reported four relaxations in amorphous trehalose.[36] Since the dc conductivity was not subtracted, there is room for ambiguity in data interpretation.[25] Given its importance as a widely occurring bioprotective, there exists an urgent need to comprehensively study the molecular mobility of amorphous trehalose. By effectively subtracting out the contribution of dc conductivity, we have demonstrated the ability to completely resolve α-relaxation even at sub-T_g temperatures. This subtraction, coupled with annealing, also enabled the identification of an excess wing, attributable to JG relaxation. This laid the foundation for the complete mapping of molecular mobility, encompassing the α- and several β-relaxations.[37]

EXPERIMENTAL SECTION

Preparation of Amorphous Trehalose. Trehalose dihydrate ($C_{12}H_{22}O_{11}\cdot 2H_2O$; Sigma, St. Louis, MO, USA; purity >99%) was used as received. Freeze-dried trehalose was obtained by lyophilization in a benchtop freeze drier (model UNITOP 400 L, Virtis, Gardiner, NY, USA). About 15 mL of aqueous trehalose solution (10% w/v) was placed in Petri dishes, cooled to −45 °C, and subjected to reduced pressure (100 mTorr). After holding the sample for 2 min at −45 °C, the temperature was slowly increased to −30 °C and primary drying was carried out for 38 h. Over the next 24 h, the temperature was gradually increased to 50 °C. The secondary drying was carried out at 50 °C for 31 h, after which the temperature was raised to 60 °C and the drying continued for 24 more hours. The samples were removed from the freeze-drier, transferred to glass containers, tightly capped and stored in a desiccator at −20 °C over anhydrous calcium sulfate (RH < 5%) until use. Further handling of the freeze-dried samples was done in a controlled humidity environment (<5% RH; in a glovebox).

Baseline Characterization of Amorphous Trehalose. Amorphous trehalose prepared by freeze-drying was found to be X-ray amorphous with a water content <0.5% w/w (determined by Karl Fischer titrimetry and thermogravimetry), and a calorimetric T_g of ∼117 °C (onset temperature).

Dynamic Dielectric Spectroscopy. Dielectric constant and dielectric loss measurements were performed with a broadband dielectric spectrometer (Novocontrol Alpha-A high performance frequency analyzer, Novocontrol Technologies, Germany). About 100 mg of sample was placed between two round copper electrodes (20 mm diameter) and a PTFE spacer. The PTFE spacer (thickness, 1 mm; area, 59.69 mm^2; capacity, 1.036 pF) was used to keep the sample confined between electrodes at high temperatures and also to minimize errors due to stray capacitance or edge effects. To study different relaxations, the dielectric measurements were carried out isothermally at various temperatures, from 30 to 170 °C, typically in the frequency range of 10^{-1} to 10^7 Hz. The sample temperature was maintained with a Novotherm temperature controller.

Analysis of Dielectric Relaxation Spectroscopy Data . The basic model describing a dielectric process is the Debye function, which considers a symmetric dielectric loss peak with a constant full width at half-maximum value of 1.14 decades. However, in most cases, the peaks of dielectric materials are much broader and often asymmetric. The Havriliak−Negami function (eq 1 but without the conductivity term) can be used to describe the symmetric and asymmetric broadening of the relaxation peaks.

RESULTS AND DISCUSSION

In order to examine the general dielectric features attributable to molecular motions in the glassy and supercooled melt of trehalose, ε'' and ε' were determined at a fixed frequency of 1 kHz, typically in temperature increments of 5 °C, over the range of 25−180 °C (temperature sweep experiment). Figure 1 is a plot of ε'' as a function of temperature, at a fixed frequency of 1 kHz. The

calorimetric T_g onset is indicated in the figure. On heating through the T_g, ε'' rapidly increased, reached a maximum and then decreased. This peak is attributed to α-relaxation, the major contributor to dielectric permittivity. Additionally, an extra "contribution" on the low temperature tail of the α-relaxation peak and a peak at ∼40 °C were observed, both attributed to two secondary relaxations. Thus, the temperature sweep experiment indicated at least three relaxations in the investigated temperature range.

Isothermal frequency sweep experiments were also conducted in the temperature range of 30−170 °C. The frequency range employed was 10^{-1}−10^{7} Hz, and the time for each measurement was ∼5 min. As the temperature was increased, at low frequencies, there was an increased contribution of dc conductivity to the dielectric loss (Figure 2).

Figure 3 is a plot of the ε'' as a function of frequency, obtained at 100 °C. The peak in the frequency range of 10^{4}−10^{5} Hz has been attributed to β_2-relaxation.[24,35] From the raw ε'' profile (filled circles), α-relaxation can be barely discerned as a curvature (pointed out in the figure) in the steeply rising region of dc conductivity. As already mentioned, earlier investigations had also pointed out this limitation.[24,25,34,35] We attempted to overcome this problem using the Kramers−Kronig relation at temperatures both above and below T_g. The T_g was determined to be ∼120 °C based on the change in temperature dependence of α-relaxation. It was possible to use the Kramers−Kronig relation since there was no contribution of interfacial polarization to the real part of dielectric permittivity (Figure 4; the small increase at low frequencies is attributed only to α-relaxation). This enabled us to calculate, over the entire frequency range, the dielectric loss values from dielectric constant data, thereby effectively eliminating the contribution of dc conductivity and completely resolving the α-relaxation peak (open circles in Figure 3). It is however recognized that the differential form of the Kramers−Kronig relation is an approximation and has some limitations.[38] The Havriliak−Negami model was used to fit the peak and obtain the average relaxation time and shape parameters (Table 1). Interestingly, an excess wing was observed on the high frequency tail of the α-relaxation peak. When the experiments were conducted at several temperatures close to but $<T_g$, the excess wing persisted. However, this feature vanished at temperatures $>T_g$ (addressed later). In an earlier report, Kaminski et al. had effectively used the Kramers−Kronig relation to investigate α-relaxation in trehalose.[25] Since their studies were limited to the supercooled liquid phase, there was no reference to the excess wing. Recently, Kwon et al. have also reported an excess wing in the dielectric profile of trehalose.[36] However, their results were obtained by fitting the dielectric loss

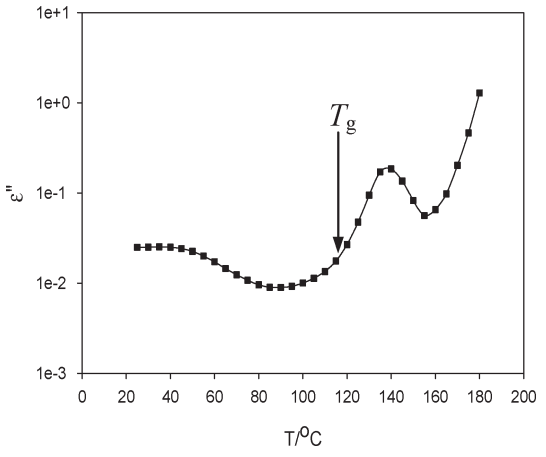

Figure 1. Plot of dielectric loss versus temperature in amorphous trehalose. The calorimetric T_g onset is shown by an arrow.

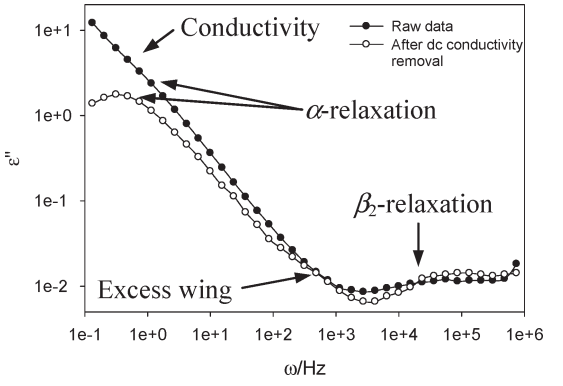

Figure 3. Dielectric loss profile of amorphous trehalose at 100 °C. Both raw ε'' profile (filled circles) and profile calculated using the Kramers−Kronig relation (open circles) are shown. Contribution from conductivity, α-relaxation and β_2-relaxation is indicated by arrows. After the removal of dc conductivity interference, α-relaxation can be clearly observed. A high frequency excess wing to the α-relaxation is also apparent.

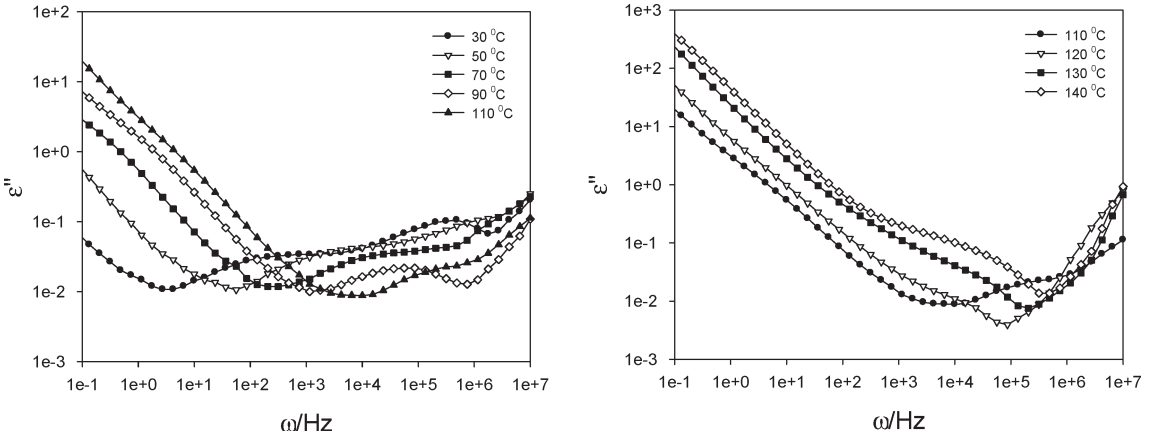

Figure 2. Isothermal dielectric profiles of amorphous trehalose over the temperature range of 30−140 °C. The contribution of dc conductivity increases at low frequencies as the temperature is increased.

data but without subtracting the contribution of dc conductivity. In light of the pronounced contribution of the conductivity, both in the regions of α-relaxation and excess wing, unambiguous modeling of the relaxation data cannot be accomplished.

This excess contribution to the high frequency region of the α-relaxation is a common feature in many glass formers, and has even served as a basis of classification of glass formers.[39] Type A glass formers are characterized by an excess wing without a well resolved β-relaxation, while type B glass formers exhibit a well-defined β-relaxation. Initially, there was a debate about the origin of this excess wing.[39−43] It was later shown, both in glycerol and in propylene carbonate, that the excess wing was indeed the high-frequency flank of the JG relaxation hidden under the α-relaxation peak.[42,43] In both the compounds, on annealing, the excess wing developed into a shoulder indicating the presence of a secondary relaxation. Due to the inability of earlier studies to observe this excess wing, trehalose was implied to be a type B glass former.[24,35] Moreover, on separate occasions, β_1- and β_2-relaxations were identified as the JG relaxation.[24,25,34] The observation of an excess wing in amorphous trehalose is potentially important. It shows, in addition to the two β-relaxations already known, the existence of another β-relaxation. The JG relaxation, involving the motion of the whole molecule, is invariably the slowest of the secondary relaxations. In the dielectric spectrum, since this excess wing occurred between α-relaxation and the already known secondary relaxations, it is hypothesized to be the JG relaxation (Figure 3). JG relaxation is believed to be a universal feature of amorphous materials and has often been viewed as a precursor to global mobility.

To completely characterize this excess wing, amorphous trehalose was annealed at 100 °C (17 °C < T_g). The isothermal dielectric profiles of samples annealed for different time periods are shown in Figure 5. Annealing for 2 h caused a pronounced shift in the α-relaxation to lower frequencies. In addition, the excess wing developed into a shoulder. Further annealing (≥4 h) facilitated the partial resolution of this hidden relaxation peak, which we termed β_3-relaxation. In trehalose, this resolution is much better than that observed in glycerol and propylene carbonate.[42,43] This partial separation enabled the use of the Havriliak−Negami model to fit the data and obtain the average relaxation time and shape parameters for this relaxation (Table 1). A representative dielectric spectrum of amorphous trehalose annealed for 8 h is shown in Figure 6. Lines represent the fitted profiles using the Havriliak−Negami model.

The β_3-relaxation peak could not be observed once the sample was heated above T_g. Heating above T_g erased the thermal history of the sample, thereby removing the effect of annealing. We had earlier pointed out that the excess wing in the unannealed trehalose could not be observed at temperatures above T_g. This is probably due to α-relaxation exhibiting much more pronounced temperature dependence than β_3-relaxation.

It is apparent from the profiles of amorphous trehalose samples annealed for 4 and 8 h that β_3-relaxation peak increased in dielectric strength as trehalose was annealed although no such effect was seen on α-relaxation (Figure 5). However, annealing for a much longer time (up to 120 h), caused an increase in the dielectric strength of α-relaxation as well (data not shown). Thus, while the dielectric strength of both β_3- and α-relaxations increase with annealing, the time required to exhibit this effect is

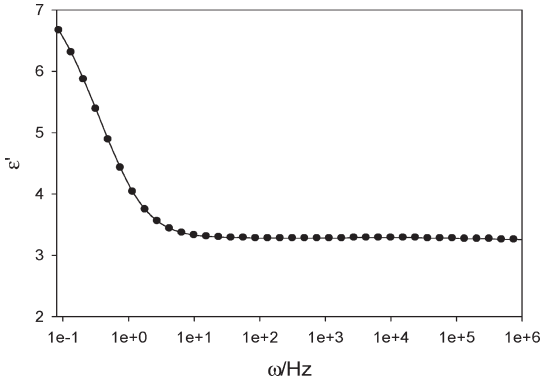

Figure 4. Dielectric constant of amorphous trehalose (at 100 °C) as a function of frequency.

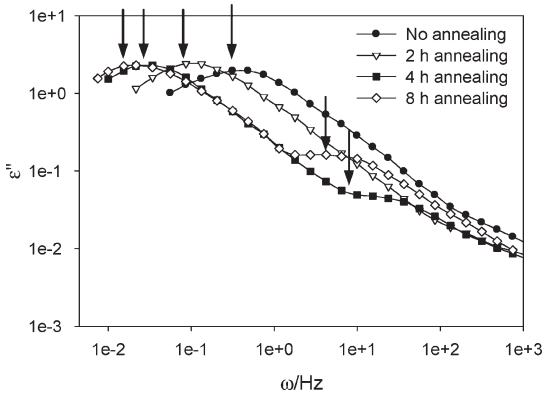

Figure 5. Isothermal dielectric relaxation profiles of different annealed samples of amorphous trehalose at 100 °C. The frequency of maximum dielectric loss (ω_{max}) is shown by arrows for the two relaxations in different samples.

Table 1. Relaxation Time for the α- and Different β-Relaxations in Amorphous Trehalose

	at 100 °C	at T_g (~120 °C)
	Unannealed Sample	
α-relaxation time (s)	0.5	0.1
	Sample Annealed for 8 h at 100 °C	
β_3-relaxation time (s)	1.2×10^{-2}	7.3×10^{-3}
Calculated independent relaxation time (τ_0) (s)[a]		3.7×10^{-3}
β_2-relaxation time (extrapolated value) (s)		8.7×10^{-8}
β_1-relaxation time (extrapolated value) (s)		1.2×10^{-8}

[a] Note that the calculated independent relaxation time (τ_0; from the extended coupling model) at T_g is close to β_3-relaxation time, but is orders of magnitude longer than β_1- and β_2-relaxation times.

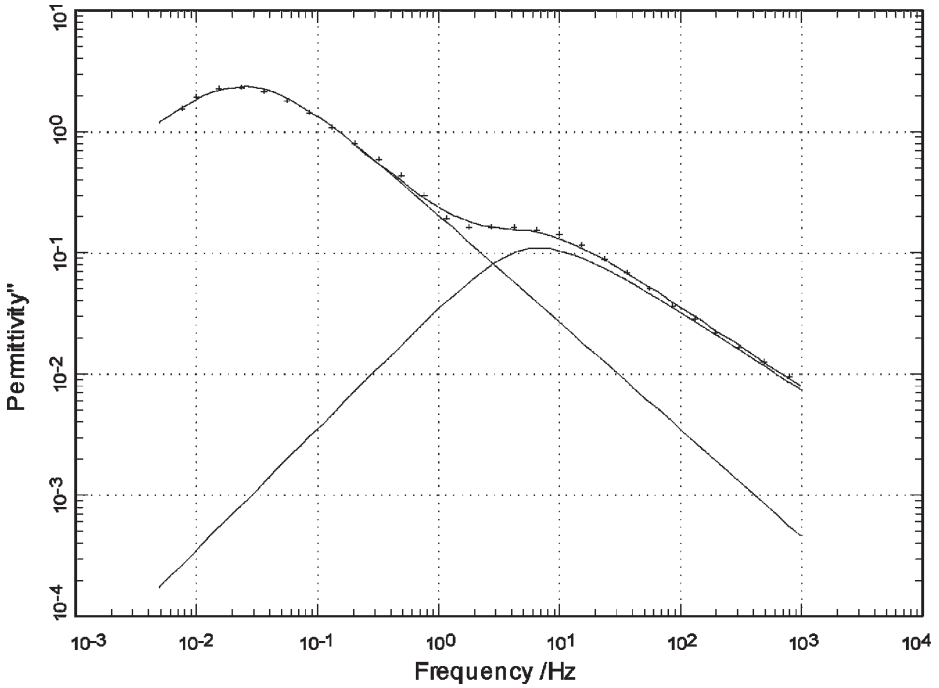

Figure 6. Isothermal dielectric relaxation profile of amorphous trehalose annealed for 8 h at 100 °C. Both α- and β_3-relaxations are simultaneously fitted using the Havriliak−Negami model to obtain the average relaxation time and shape parameters.

very different. On the other hand, the frequency of maximum loss (ω_{max}) very quickly shifted to lower values (i.e., longer relaxation time) for α-relaxation, while this effect was just discernible (the ω_{max} values for the 4 and 8 h of annealing time are pointed out in Figure 5) for the β_3-relaxation peak. Thus qualitatively, annealing has a similar effect on both β_3- and α-relaxations, suggesting that β_3 is the true JG relaxation. In light of the potential importance of this observation, the effect of annealing time will be the subject of a separate publication.

Ngai proposed an extending coupling model, wherein JG relaxations (also referred to as independent relaxations) are considered as precursors to α-relaxation.[16] The two relaxations are related by a temperature independent "crossover time", τ_c. At times shorter than τ_c, JG relaxations are prevalent, and at times longer than τ_c, these are transformed into the slower cooperative α-relaxation. For most amorphous glass formers, τ_c is ∼2 ps.[17,44,45] In an effort to further check if β_3-relaxation is the JG relaxation, the independent relaxation time, τ_0, was calculated for the 8 h annealed sample using the coupling model by Ngai:[16,17]

$$\tau_0 = \tau_\alpha^{\beta_{KWW}} \times \tau_c^{(1-\beta_{KWW})} \quad (4)$$

where τ_α is the α-relaxation time at T_g and β_{KWW} is the measure of the deviation from exponential decay of the α-relaxation time in the Kohlrausch−Williams−Watts (KWW) equation. Both were calculated from the experimentally obtained α-relaxation parameters (see Supporting Information).[46] This was done to compare the calculated value of τ_0 with the experimentally determined value of β_3-relaxation at T_g (Table 1). The sample annealed for 8 h proved to be ideal for this purpose since the β_3-relaxation was sufficiently resolved. The β_1- and β_2-relaxation times at T_g, calculated using the Arrhenius equation (see Supporting Information), were much shorter than τ_0, indicating that neither of them correlated to α-relaxation (Table 1). On the other hand, the calculated value of τ_0 and the measured value of β_3-relaxation at T_g were in good agreement establishing the relationship of this secondary relaxation with the cooperative α-relaxation, and supporting our hypothesis that it is the JG relaxation.

In summary, at temperatures below but close to T_g, subtraction of dc conductivity permitted not only the resolution of α-relaxation but also the identification of an excess wing in the dielectric spectrum of amorphous trehalose. Annealing, at a temperature close to T_g, resulted in the development of this excess wing into an unresolved relaxation peak which could be successfully analyzed to determine its relaxation parameters. This relaxation peak, due to its position in the dielectric spectra, its similarity in annealing time dependence to α-relaxation, and its good agreement with the calculated independent relaxation time, could be assigned to the JG process.

This work shows that, in order to successfully identify all the mobility features in the dielectric spectra, it is necessary to unambiguously study the relaxation profiles of amorphous materials at different temperatures. In case of disaccharides where there is considerable interference from dc conductivity, annealing coupled with the Kramers−Kronig approach could be very successful in identifying hidden but potentially important relaxation modes. This approach enabled the identification of JG relaxation, which can be of great practical importance in light of its potential impact on the stability of amorphous compounds.

■ ASSOCIATED CONTENT

Supporting Information. Calculation of the extrapolated values of β_1- and β_2-relaxation times at T_g and calculation of the independent relaxation time from the α-relaxation peak. This material is available free of charge via the Internet at http://pubs.acs.org.

AUTHOR INFORMATION

Corresponding Author

*Department of Pharmaceutics, University of Minnesota, Minneapolis, Minnesota 55455, USA. Phone: 612-624-9626. Fax: 612-626-2125. E-mail: surya001@umn.edu.

ACKNOWLEDGMENT

We thank Brad L. Givot (3M, St. Paul, MN) for all his help and support during the course of the project and 3M (St. Paul, MN) for providing us generous access to the dielectric spectrometer. Marcus T. Cicerone (NIST, Gaithersburg, MD) is thanked for his insightful comments. Partial support was provided by the William and Mildred Peters Endowment Fund. We thank the reviewers for enabling significant improvements in the manuscript.

REFERENCES

(1) Hancock, B. C.; Zografi, G. Characteristics and Significance of the Amorphous State in Pharmaceutical Systems. *J. Pharm. Sci.* **1997**, *86*, 1–12.

(2) Johari, G. P.; Kim, S.; Shanker, R. M. Dielectric Relaxation and Crystallization of Ultraviscous Melt and Glassy States of Aspirin, Ibuprofen, Progesterone, and Quinidine. *J. Pharm. Sci.* **2007**, *96*, 1159–1175.

(3) Johari, G. P.; Kim, S.; Shanker, R. M. Dielectric Study of Equimolar Acetaminophen−Aspirin, Acetaminophen−Quinidine, and Benzoic Acid−Progesterone Molecular Alloys in the Glass and Ultraviscous States and Their Relevance to Solubility and Stability. *J. Pharm. Sci.* **2010**, *99*, 1358–1374.

(4) Bhugra, C.; Rambhatla, S.; Bakri, A.; Duddu, S. P.; Miller, D. P.; Pikal, M. J.; Lechuga-Ballesteros, D. Prediction of the Onset of Crystallization of Amorphous Sucrose below the Calorimetric Glass Transition Temperature from Correlations with Mobility. *J. Pharm. Sci.* **2007**, *96*, 1258–1269.

(5) Bhugra, C.; Shmeis, R.; Krill, S. L.; Pikal, M. J. Prediction of Onset of Crystallization from Experimental Relaxation Times. II. Comparison between Predicted and Experimental Onset Times. *J. Pharm. Sci.* **2008**, *97*, 455–472.

(6) Aso, Y.; Yoshioka, S.; Kojima, S. Molecular Mobility-Based Estimation of the Crystallization Rates of Amorphous Nifedipine and Phenobarbital in Poly(vinylpyrrolidone) Solid Dispersions. *J. Pharm. Sci.* **2004**, *93*, 384–391.

(7) Sixou, B.; Faivre, A.; David, L.; Vigier, G. Intermolecular and Intramolecular Contributions to the Relaxation Process in Sorbitol and Maltitol. *Mol. Phys.* **2001**, *99*, 1845–1850.

(8) Paluch, M.; Pawlus, S.; Hensel-Bielowka, S.; Kaminski, K.; Psurek, T.; Rzoska, S. J.; Ziolo, J.; Roland, C. M. Effect of Glass Structure on the Dynamics of the Secondary Relaxation in Diisobutyl and Diisoctyl Phthalates. *Phys. Rev. B* **2005**, *72*, 224205.

(9) Johari, G. P.; Goldstein, M. Viscous Liquids and the Glass Transition. II. Secondary Relaxations in Glasses of Rigid Molecules. *J. Chem. Phys.* **1970**, *53*, 2372–2388.

(10) Vyazovkin, S.; Dranca, I. Effect of Physical Aging on Nucleation of Amorphous Indomethacin. *J. Phys. Chem. B* **2007**, *111*, 7283–7287.

(11) Alie, J.; Menegotto, J.; Cardon, P.; Duplaa, H.; Caron, A.; Lacabanne, C.; Bauer, M. Dielectric Study of the Molecular Mobility and the Isothermal Crystallization Kinetics of an Amorphous Pharmaceutical Drug Substance. *J. Pharm. Sci.* **2004**, *93*, 218–233.

(12) Hikima, T.; Adachi, Y.; Hanaya, M.; Oguni, M. Determination of Potentially Homogeneous-Nucleation-Based Crystallization in *O*-Terphenyl and an Interpretation of the Nucleation-Enhancement Mechanism. *Phys. Rev. B* **1995**, *52*, 3900–3908.

(13) Hikima, T.; Hanaya, M.; Oguni, M. Microscopic Observation of a Peculiar Crystallization in the Glass Transition Region and β-Process as Potentially Controlling the Growth Rate in Triphenylethylene. *J. Mol. Struct.* **1999**, *479*, 245–250.

(14) Johari, G. P. Localized molecular motions of β-relaxation and its energy landscape. *J. Non-Cryst. Solids* **2002**, *307−310*, 317–325.

(15) Vij, J. K.; Power, G. Physical ageing and the Johari−Goldstein relaxation in molecular glasses. *J. Non-Cryst. Solids* **2011**, *357*, 783–792.

(16) Ngai, K. L. An Extended Coupling Model Description of the Evolution of Dynamics with Time in Supercooled Liquids and Ionic Conductors. *J. Phys.: Condens. Matter* **2003**, *15*, S1107–S1125.

(17) Ngai, K. L. Relation between Some Secondary Relaxations and the α Relaxations in Glass-Forming Materials According to the Coupling Model. *J. Chem. Phys.* **1998**, *109*, 6982–6994.

(18) Weuts, I.; Kempen, D.; Six, K.; Peeters, J.; Verreck, G.; Brewster, M.; Van den Mooter, G. Evaluation of Different Calorimetric Methods to Determine the Glass Transition Temperature and Molecular Mobility below T_g for Amorphous Drugs. *Int. J. Pharm.* **2003**, *259*, 17–25.

(19) Surana, R.; Pyne, A.; Rani, M.; Suryanarayanan, R. Measurement of Enthalpic Relaxation by Differential Scanning Calorimetry-Effect of Experimental Conditions. *Thermochim. Acta* **2005**, *433*, 173–182.

(20) Andronis, V.; Zografi, G. Molecular Mobility of Supercooled Amorphous Indomethacin Determined by Dynamic Mechanical Analysis. *Pharm. Res.* **1997**, *14*, 410–414.

(21) Aso, Y.; Yoshioka, S.; Kojima, S. Relationship between the Crystallization Rates of Amorphous Nifedipine, Phenobarbital, and Flopropione, and their Molecular Mobility as Measured by their Enthalpy Relaxation and ^{1}H NMR Relaxation Times. *J. Pharm. Sci.* **2000**, *89*, 408–416.

(22) Kremer, F.; Schonhals, A. *Broadband Dielectric Spectroscopy*; Springer-Verlag: New York, 2003; pp 99−129.

(23) Ngai, K. L.; Casalini, R.; Capaccioli, S.; Paluch, M.; Roland, C. M. Dispersion of the Structural Relaxation and the Vitrification of Liquids. In *Fractals, Diffusion, and Relaxation in Disordered Complex Systems: Advances in Chemical Physics, Part B*; Coffey, W. T., Kalmykov, Y. P., Eds.; John Wiley & Sons, Inc.: Hoboken, 2006; Vol. 133, pp 497−594.

(24) De Gusseme, A.; Carpentier, L.; Willart, J. F.; Descamps, M. Molecular Mobility in Supercooled Trehalose. *J. Phys. Chem. B* **2003**, *107*, 10879–10886.

(25) Kaminski, K.; Kaminska, E.; Wlodarczyk, P.; Pawlus, S.; Kimla, D.; Kasprzycka, A.; Paluch, M.; Ziolo, J.; Szeja, W.; Ngai, K. L. Dielectric Studies on Mobility of the Glycosidic Linkage in Seven Disaccharides. *J. Phys. Chem. B* **2008**, *112*, 12816–12823.

(26) Kaminski, K.; Kaminska, E.; Hensel-Bielowka, S.; Pawlus, S.; Paluch, M.; Ziolo, J. High Pressure Study on Molecular Mobility of Leucrose. *J. Chem. Phys.* **2008**, *129*, 084501.

(27) Lynch, A. C. Relationship between Permittivity and Loss Tangent. *Proc. IEE* **1971**, *118*, 244–246.

(28) Crowe, J. H.; Crowe, L. M.; Carpenter, J. F.; Aurell Wistrom, C. Stabilization of Dry Phospholipid Bilayers and Proteins by Sugars. *Biochem. J.* **1987**, *242*, 1–10.

(29) Leslie, S. B.; Israeli, E.; Lighthart, B.; Crowe, J. H.; Crowe, L. M. Trehalose and Sucrose Protect Both Membranes and Proteins in Intact Bacteria during Drying. *Appl. Environ. Microbiol.* **1995**, *61*, 3592–3597.

(30) Crowe, J. H.; Carpenter, J. F.; Crowe, L. M. The Role of Vitrification in Anhydrobiosis. *Annu. Rev. Physiol.* **1998**, *60*, 73–103.

(31) Sundaramurthi, P.; Suryanarayanan, R. Trehalose Crystallization during Freeze-Drying: Implications on Lyoprotection. *J. Phys. Chem. Lett.* **2010**, *1*, 510–514.

(32) Sundaramurthi, P.; Patapoff, T. W.; Suryanarayanan, R. Crystallization of Trehalose in Frozen Solutions and its Phase Behavior during Drying. *Pharm. Res.* **2010**, *27*, 2374–2383.

(33) Lefort, R.; Bordat, P.; Cesaro, A.; Descamps, M. Exploring the Conformational Energy Landscape of Glassy Disaccharides by Cross Polarization Magic Angle Spinning ^{13}C Nuclear Magnetic Resonance and Numerical Simulations. II. Enhanced Molecular Flexibility in Amorphous Trehalose. *J. Chem. Phys.* **2007**, *126*, 014511.

(34) Moura Ramos, J. J.; Pinto, S. S.; Diogo, H. P. The Slow Molecular Mobility in Amorphous Trehalose. *ChemPhysChem* **2007**, *8*, 2391–2396.

(35) Cummins, H. Z.; Zhang, H.; Oh, J.; Seo, J.-A.; Kim, H. K.; Hwang, Y.-H.; Yang, Y. S.; Yu, Y. S.; Inn, Y. The Liquid−Glass

Transition in Sugars: Relaxation Dynamics in Trehalose. *J. Non-Cryst. Solids* **2006**, *352*, 4464–4474.

(36) Kwon, H.; Seo, J.; Kim, H. K.; Hwang, Y. Study of Dielectric Relaxations of Anhydrous Trehalose and Maltose Glasses. *J. Chem. Phys.* **2011**, *134*, 014508.

(37) Bhardwaj, S. P.; Givot, B. L.; Suryanarayanan, R. Global Molecular Mobility in Amorphous Trehalose and the Effect of Annealing. *AAPS J.* **2010**, *12*, S2.

(38) Wübbenhorst, M.; Turnhout, J. Analysis of Complex Dielectric Spectra. I. One-Dimensional Derivative Techniques and Three-Dimensional Modelling. *J. Non-Cryst. Solids* **2002**, *305*, 40–49.

(39) Wiedersich, J.; Blochowicz, T.; Benkhof, S.; Kudlik, A.; Surovtsev, N. V.; Tschirwitz, C.; Novikov, V. N.; Rössler, E. Fast and Slow Relaxation Processes in Glasses. *J. Phys.: Condens. Matter* **1999**, *11*, A147–A156.

(40) León, C.; Ngai, K. L.; Roland, C. M. Relationship between the Primary and Secondary Dielectric Relaxation Processes in Propylene Glycol and its Oligomers. *J. Chem. Phys.* **1999**, *110*, 11585–11591.

(41) León, C.; Ngai, K. L. Rapidity of the Change of the Kohlrausch Exponent of the α-Relaxation of Glass-Forming Liquids at T_B or T_β and Consequences. *J. Phys. Chem. B* **1999**, *103*, 4045–4051.

(42) Schneider, U.; Brand, R.; Lunkenheimer, P.; Loidl, A. Excess Wing in the Dielectric Loss of Glass Formers: A Johari-Goldstein β Relaxation?. *Phys. Rev. Lett.* **2000**, *84*, 5560–5563.

(43) Lunkenheimer, P.; Wehn, R.; Riegger, T.; Loidl, A. Excess Wing in the Dielectric Loss of Glass Formers: Further Evidence for a β-Relaxation. *J. Non-Cryst. Solids* **2002**, *307*−*310*, 336–344.

(44) Colmenero, J.; Arbe, A.; Alegría, A. Crossover from Debye to Non-Debye Dynamical Behavior of the α Relaxation Observed by Quasielastic Neutron Scattering in a Glass-Forming Polymer. *Phys. Rev. Lett.* **1993**, *71*, 2603–2606.

(45) Colmenero, J.; Arbe, A.; Alegría, A. The Dynamics of the α- and β-Relaxations in Glass-Forming Polymers Studied by Quasielastic Neutron Scattering and Dielectric Spectroscopy. *J. Non-Cryst. Solids* **1994**, *172*−*174*, 126–137.

(46) Alvarez, F.; Alegría, A.; Colmenero, J. Relationship between the Time-Domain Kohlrausch-Williams-Watts and Frequency-Domain Havriliak-Negami Relaxation Functions. *Phys. Rev. B* **1991**, *44*, 7306–7312.